A.C.-d.c. load flows with realistic representation of the convertor plant

Prof. J. Arrillaga, M.Sc.Tech., Ph.D., C.Eng., F.I.E.E., and P. Bodger, B.E.

Indexing terms: Power convertors, Electric load, D.C. power transmission

Abstract

H.V. d.c. convertor stations contain a.c. plant components which are specified by their relationship with d.c. link parameters and cannot be represented in conventional terms within the a.c. load-flow solutions. In the paper a comprehensive d.c. link model is developed with generality to represent all the plant components and operating conditions encountered in practice. The New Zealand a.c.-d.c.-a.c. scheme is used as a test system, and the results show that a unified fast-decoupled load-flow solution of two and three a.c. systems interconnected by the d.c. link converges for all practical operating conditions without increasing the number of iterations.

List of principal symbols

$V\angle\theta$ = nodal voltage (phase angle referred to slack node)
$E\angle\phi$ = convertor alternating voltage
$V\angle\psi$ = nodal voltage (phase angle referred to convertor current)
V_d = direct voltage
I = alternating current
I_d = direct current
$IL\omega_m$ = alternating current (phase angle referred to convertor current on adjacent pole)
a, t = transformer ratios
X = reactance
B = susceptance
α = convertor control angle
R_{dc} = d.c. line resistance
R = d.c. residual
x = d.c. link variable
P = active power
Q = reactive power
X_m, X_n = commutation reactances

1 Introduction

Several papers have described the incorporation of h.v. d.c. links within a.c. load-flow programmes either as an integral part of the a.c. iterative procedure[1] or as a sequential solution.[2, 3] These models have emphasised the simplicity of their d.c.-link representation, its adaptability to different types of load-flow solution and the small effect that its inclusion has on the number of iterations and the overall computer requirements.

The minimum numbers of variables required to represent a basic two-terminal link with on-load tap-changing two-winding transformers and under perfectly symmetrical bipolar operation has been shown to be 13 (Reference 4), four of which have to be fixed in advance as control specifications. In practice, however, the configuration and control characteristics of the convertor interface is more complex and requires further variables and equations.

A survey of existing schemes clearly indicates that no model can be applied generally. Furthermore, no one of the existing schemes can be properly represented by the models so far presented in the literature. From the survey, the New Zealand a.c.-d.c.-a.c. system has the required generality in terms of d.c.-related plant components and operating characteristics. The N.Z. d.c. link interconnects two separate a.c. systems of comparable capacities and under the same authority. It has two- and three-winding transformers with tap-change capability, synchronous compensators connected to tertiary windings, and filters connected to primary and tertiary windings. Power can be fed into the link from two separate generating busbars or from the a.c. system. The link can operate in both directions and in monopolar or bipolar modes and with common or independent controls.

The development of a unified load flow based on the N.Z. system and applicable to existing schemes is described in this paper. The feasibility of a unified fast-decoupled a.c.-d.c. solution has already been demonstrated[5] for a basic d.c. link interconnecting two nodes of an a.c. power system. The present model uses a modified fast-decoupled algorithm that includes more than one a.c. system, and an enlarged d.c. model with realistic representation of the a.c.-d.c. terminals.

Paper 8020 P, first received 4th April and in revised form 23rd August 1977

Prof. Arrillaga is with the Department of Electrical Engineering, University of Canterbury, Christchurch, New Zealand, and Mr. Bodger is with the New Zealand Electricity Department

Table 1
CHARACTERISTICS OF NEW ZEALAND D.C. LINK

(*a*) Transformer data	Benmore interconnecting	Benmore convertor	Haywards convertor
Top-tap ratio, %	16·67	2·5	2·5
Bottom-tap ratio, %	−13·33	−2·5	−2·5
Number of tap positions	18	3	3
Reactance (2-winding)		0·0308	
Primary reactance	0·0460		0·0265
Secondary reactance	0·0206		−0·0014
Tertiary reactance	− 0·0045		0·0176

	Benmore		Haywards
(*b*) Convertor data	pole 1	pole 2	
Commutation reactance*	0·0897	0·0897	0·0762
Number of bridges	2	2	4
Minimum control angle, degrees	10	10	11
Terminal busbar filter susceptance			1·1
Benmore filter susceptance	0·5	0·5	

D.C. link resistance = 25·56 Ω. This includes resistance of line, cables and smoothing reactors
Maximum link current = 1200 A
*Sample reactance with three machines on each Benmore generating bus
Base power = 100 MVA
Base voltages: Benmore: 98·5 kV, Haywards: 110 kV, d.c. line: 98·5 kV

2 System under consideration

A simplified diagram of the New Zealand h.v. d.c. interconnection is illustrated in Fig. 1, and relevant information is given in Table 1.

A complete set of variables necessary to provide the operational flexibility required from the d.c. link is shown in Fig. 2 and an equivalent circuit suitable for the load-flow analysis is shown in Fig. 3. This Figure may give the impression that the d.c. link has been extended unnecessarily into the a.c. system at the Benmore end, as any plant beyond the convertor transformer can normally be more easily included in the a.c. system.

However, under most loading conditions the interconnecting transformer taps become a function of the d.c. link power transfer. Moreover, the various nodes appearing in Fig. 3 are not always specified in a manner suitable for inclusion within standard a.c. load flows (i.e. P, V or P, Q representations); instead they may be specified by direct or indirect relationships with d.c. link-control parameters as will be explained in Section 3.1. Finally, under certain operating conditions, also described in Section 3.1, the a.c. systems connected to each pole at the Benmore end will contain different items of plant.

The following notes will help to explain the operating characteristics of the d.c. link under consideration:

(*a*) Under all steady-state operating conditions with northward transmission the terminal a.c. busbar voltage at Haywards is held constant by the action of synchronous compensators on the tertiaries of the convertor transformers. The convertor transformer taps are normally kept constant at both ends. The generator busbar voltages at Benmore are adjusted to give constant control angles at both convertors and specified power through each pole of the link. To match these voltages to the South Island a.c. network via the Benmore 220 kV busbar, the interconnecting transformers have an on-load tap-changing facility.

0020–3270/78/8020–0041 $1·50/0

(*b*) Under peak system load conditions, both Benmore 16 kV busbars have real and reactive power generation.

(*c*) Under light-load conditions, the Benmore machines have the facility to operate as synchronous compensators. This is obtained by depressing the tailwater with compressed air, and provides an immediate acting spinning reserve. Depending on the loading, (i) neither, (ii) one or (iii) both busbars may have machines in service. With southward transmission, the Benmore machines are used as synchronous compensators.

3 D.C.-system equations

With reference to Fig. 3 the following relationships can be written between the voltages on the a.c. and d.c. sides of the convertor, as derived from the power equalities:

$$V_{dm1} = K_1 E_{m1} \cos \phi_{m1} \quad (1)$$

$$V_{dm1} = K_1 E_{m2} \cos (\phi_{m2} - \omega_{m2}) \quad (2)$$

$$V_{dn} = K_1' E_n \cos \phi_n \quad (3)$$

and similarly, for the currents,

$$I_{m1} = K_1 I_d$$

$$I_{m2} = K_1 I_d$$

$$I_n = K_1' I_d$$

The convertor a.c. currents are taken as phase references for the d.c.-model variables. In general, at the Benmore end only one pole can be used as a reference to cope with unbalanced-pole operating conditions. For convenience ω_{m2} is included in the equations but the choice of reference pole is arbitrary.

Six equations can be written relating the real and imaginary currents flowing into the convertors from the transformers:

$$K_1 I_d = a_{m1} B_m (a_{m1} E_{m1} \sin \phi_{m1} - V_{m1} \sin \psi_{m1}) \quad (4)$$

$$0 = a_{m1} V_{dm1} - K_1 V_{m1} \cos \psi_{m1} \quad (5)$$

$$K_1 I_d \cos \omega_{m2} = a_{m2} B_m (a_{m2} E_{m2} \sin \phi_{m2} - V_{m2} \sin \psi_{m2}) \quad (6)$$

$$K_1 I_d \sin \omega_{m2} = -a_{m2} B_m (a_{m2} E_{m2} \cos \phi_{m2} - V_{m2} \cos \psi_{m2}) \quad (7)$$

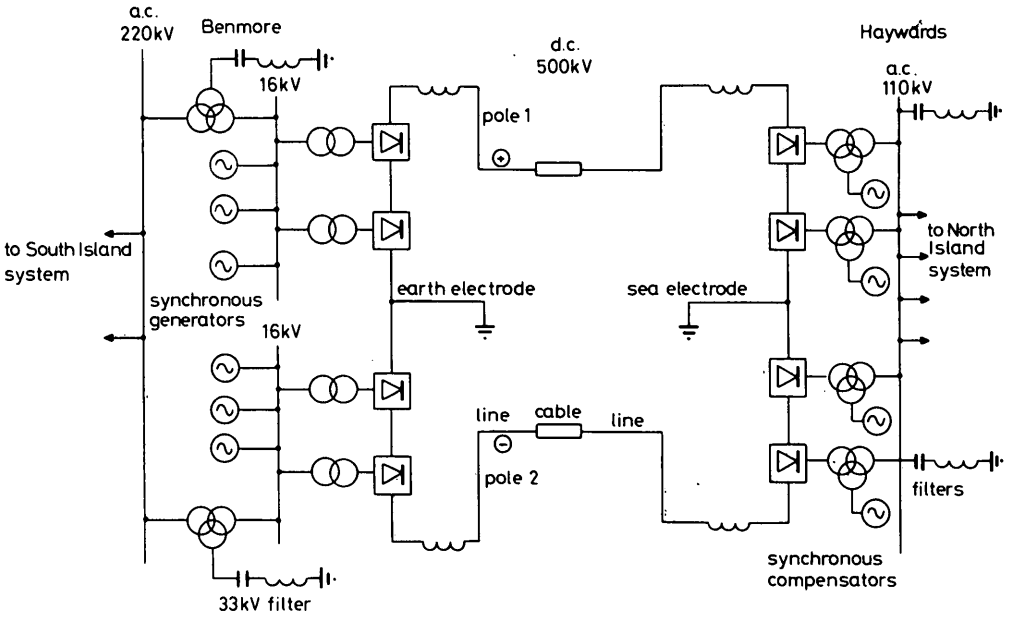

Fig. 1
Simplified diagram of the New Zealand h.v. d.c. interconnection

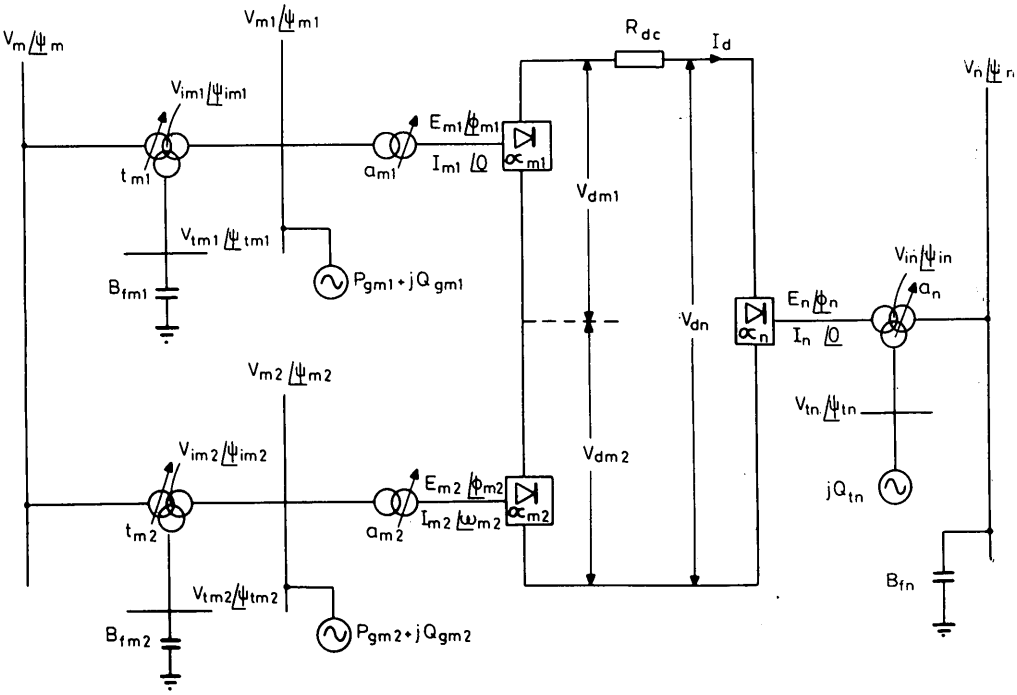

Fig. 2
Convenient representation of the New Zealand h.v. d.c. interconnection providing complete operational flexibility

$$K_1' I_d = -B_{sn}(E_n \sin \phi_n - V_{in} \sin \psi_{in}) \quad (8)$$

$$0 = V_{dn} - K_1' V_{in} \cos \psi_{in} \quad (9)$$

Eqns. 5 and 9 are expressed in terms of the direct voltage as obtained from eqns. 1 and 3.

There are four equations which relate the direct voltages and currents:

$$V_{dm1} = K_1 E_{m1} \cos \alpha_{m1} - K_2 X_{m1} I_d \quad (10)$$

$$V_{dm2} = K_1 E_{m2} \cos \alpha_{m2} - K_2 X_{m2} I_d \quad (11)$$

$$V_{dn} = K_1' E_n \cos \alpha_n - K_2' X_n I_d \quad (12)$$

$$R_{dc} I_d = V_{dm1} + V_{dm2} - V_{dn} \quad (13)$$

Six more equations, eqns. 14–19, not written out here, are derived from the real and reactive power mismatches at the intermediate nodes of the three-winding transformers and five equations, eqns. 20–24, not written out here, from the real power mismatches at the tertiary busbars and the Benmore generator busbars.

The remaining are specified control equations (discussed in Section 3.1) which depend on the nature of operation of the h.v. d.c. link and on the equipment connected to the tertiaries of the three-winding transformers.

3.1 Control specifications

13 control equations are required to give a total system description of 37, corresponding to the number of d.c.-link variables. With regard to the operational modes of the New Zealand link, as described in Section 2, the following equations can be written for all cases:

(*a*) control angles are specified:

$$\cos \alpha_{m1}^{sp} - \cos \alpha_{m1} = 0 \quad (25)$$

$$\cos \alpha_{m2}^{sp} - \cos \alpha_{m2} = 0 \quad (26)$$

$$\cos \alpha_n^{sp} - \cos \alpha_n = 0 \quad (27)$$

(*b*) convertor transformer taps are manually set:

$$a_{m1}^{sp} - a_{m1} = 0 \quad (28)$$

$$a_{m2}^{sp} - a_{m2} = 0 \quad (29)$$

$$a_n^{sp} - a_n = 0 \quad (30)$$

(*c*) three equations relate to the system elements on the tertiaries of the three-winding transformers. At Benmore, only filters (passive elements) are connected and hence reactive-power mismatches are available, while at Haywards, synchronous compensators maintain the terminal voltage:

$$\Delta Q_{tm1}/V_{tm1} = 0 \quad (31)$$

$$\Delta Q_{tm2}/V_{tm2} = 0 \quad (32)$$

$$V_n^{sp} - V_n = 0 \quad (33)$$

(*d*) the power transfer through each pole of the d.c. link is specified:

$$P_{dm1} = V_{dm1} I_d \quad (34)$$

$$P_{dm2} = V_{dm2} I_d \quad (35)$$

(*e*) the remaining two equations depend on the availability of generation at Benmore under peak, light or power-reversal operating conditions. This is intimately related to the interconnecting transformer taps and the specification of the Benmore 220 kV voltage.

(i) With real and reactive power generation on both Benmore 16 kV busbars:

If V_m is specified the interconnecting taps are made equal to reduce circulating reactive volt amperes between poles, and the equations are

$$t_{m1} - t_{m2} = 0 \quad (36a)$$

$$V_m^{sp} - V_m = 0 \quad (37a)$$

If V_m is not specified, the taps are determined by a.c.-system considerations and must be specified *a priori*; hence

$$t_{m1}^{sp} - t_{m1} = 0 \quad (36b)$$

$$t_{m2}^{sp} - t_{m2} = 0 \quad (37b)$$

(ii) For generation or synchronous-condenser operation on the Benmore 16 kV busbar 1 only, a reactive-power mismatch is available for busbar 2; i.e.

$$\Delta Q_{m2}/V_{m2} = 0 \quad (36c)$$

The remaining equation is either

$$V_m^{sp} - V_m = 0 \quad (37c)$$

or $$t_{m1}^{sp} - t_{m1} = 0$$

depending on whether the terminal busbar voltage is specified or left free. For generation on busbar 2 only, subscripts 1 and 2 should be interchanged.

(iii) When there are no machines available at Benmore, the terminal voltage cannot be maintained. Reactive-power mismatches can then be specified for both generator busbars, and the interconnecting taps are freed.

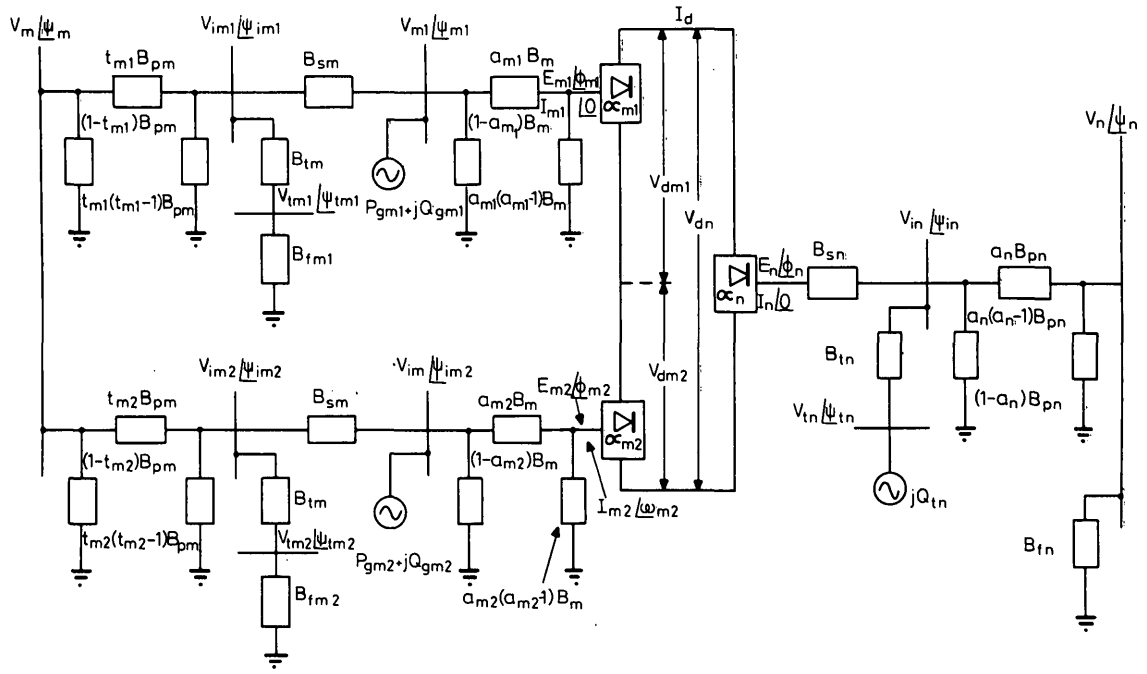

Fig. 3
Mathematically equivalent model of the link suitable for load-flow analysis

$$\Delta Q_{m1}/V_{m1} = 0 \quad (36d)$$

$$\Delta Q_{m2}/V_{m2} = 0 \quad (37d)$$

The set of eqns. 1–37 specify the New Zealand h.v. d.c. link under general operating conditions and transmission north. They apply equally well for southward transmission, in which power transfer is specified as negative in eqns. 34 and 35. The change in the sign of the d.c. voltages is most easily dealt with in the constants K_1, K_1', K_2 and K_2'. Eqn. 33 is replaced by

$$V_{dn}^{sp} - V_{dn} = 0$$

since this direct voltage is held constant.

Under constant-current control, equal power transfer per pole is assumed, and eqns. 34 and 35 are replaced by

$$I_d^{sp} - I_d = 0$$

$$V_{dm1} - V_{dm2} = 0$$

4 Unified load-flow solution

With reference to the fast-decoupled algorithm,[6] the following interface equations can be written for conditions at the convertor terminals for the various operating conditions outlined in Section 3.1:

(*a*) real-power mismatches

$$\Delta P_m/V_m = 0 \text{ (for variable } \theta_m)$$

$$\Delta P_n/V_n = 0 \text{ (for variable } \theta_n)$$

(*b*) reactive-power mismatches

$$\Delta Q_m/V_m = 0 \text{ (for variable } V_m)$$

$$\Delta Q_n/V_n = 0 \text{ (for variable } V_n)$$

The residuals $[R]$ for the 37 nonlinear equations of the d.c. link can be expressed in terms of a Jacobian submatrix $[A]$ and the d.c. link variables $[x]$, i.e. $R = A\Delta x$

The 37 equations describing the d.c. link are ordered in Appendix 10 to achieve a better-conditioned A matrix. The diagonal elements up to row 20 are always present and their magnitudes are large compared to the off-diagonal terms. Therefore it is necessary to test for the largest pivot element only from the 21st row, and computing time is thus saved without significant inaccuracy due to round-off error.

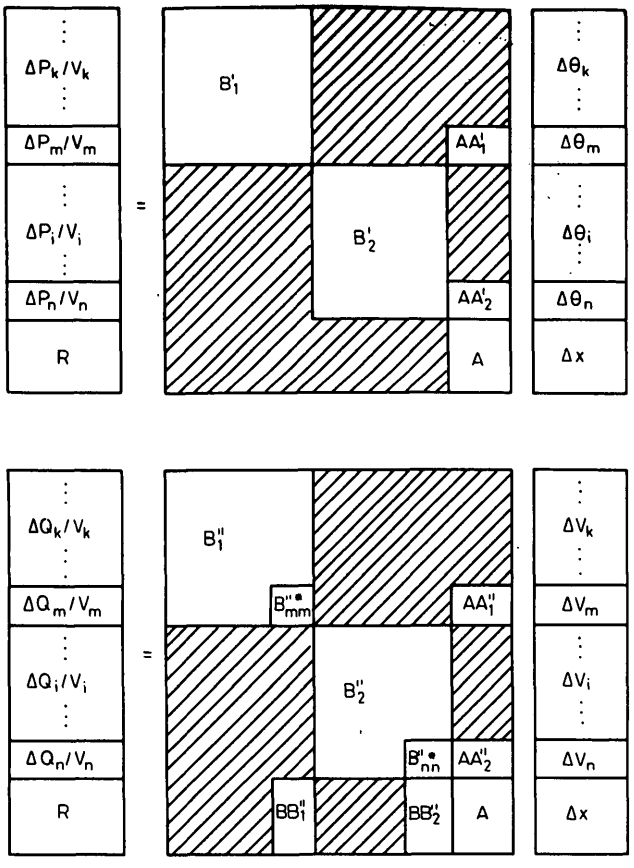

Fig. 4
General Jacobian matrix equations

As the two a.c. systems are not synchronously connected each has its own slack busbar. The structure of the combined a.c.-d.c.-a.c. Jacobian matrix equations is shown in Fig. 4, where

(i) subscript k denotes elements of a.c. system 1, and $k \neq m$

(ii) subscript i denotes elements of a.c. system 2 and $i \neq n$

(iii) shaded areas denote zero elements

5 Three-terminal operation

There exists a further mode of operation in which the Benmore 16 kV busbars are isolated from the South Island system and the generators feed power directly to North Island via the d.c. link. This constitutes a three-terminal configuration as illustrated in Fig. 5 and can be modelled by the following 23 equations:

(*a*) Eqns. 1 to 13 as before, but with the following modifications:

(i) $\omega_{m2} = 0$

because the independence of convertor terminals permits the use of each a.c. value as a reference for its respective terminal.

(ii) Eqn. 7 is combined with eqn. 2 to produce:

$$0 = a_{m2} V_{dm2} - K_1 V_{m2} \cos \psi_{m2}$$

(*b*) Three further equations resulting from the real- and reactive-power mismatches at the intermediate busbar of the Haywards convertor transformer and the real-power mismatch at the tertiary busbar.

(*c*) Equations. 25–30 and eqn. 33.

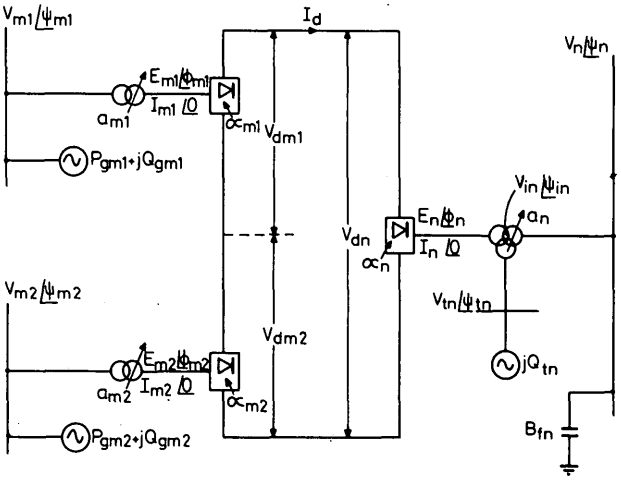

Fig. 5
Three-terminal operation

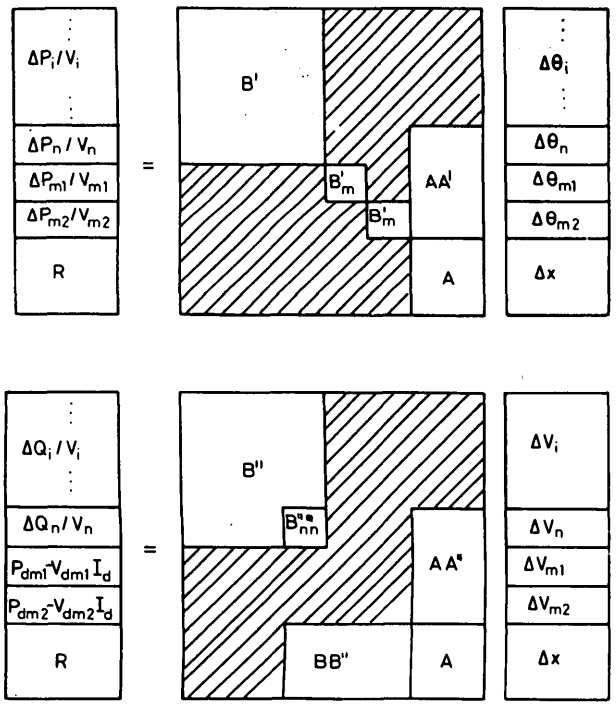

Fig. 6
Jacobian matrix equations for three-terminal operation

Table 2
SUMMARY OF OPERATIONAL MODES TESTED ON A BURROUGHS B6718 DIGITAL COMPUTER

Case	Number of iterations	Specified controls						Generation at Benmore	
		P_{dm1}	P_{dm2}	t_{m1}	t_{m2}	V_m	other	pole 1	pole 2
1	$3\frac{1}{2}$	300	300	√	√			√	√
2	3	300	300			√		√	√
3	$3\frac{1}{2}$	280	320	√	√			√	√
4	3	320	280			√		√	√
5	4	100	100						
6	4	100	100	√				√	
7	4	100	100		√				√
8	4	100	100			√			√
9	4	100	100	√	√		V_n specified	√	√
10	4	100	100			√		√	√
11	$3\frac{1}{2}$	120	80	√				√	
12	4	120	80			√			√
13	$4\frac{1}{2}$	−100	−100	√	√			√	√
14	$3\frac{1}{2}$	−100	−100	√	√		V_{dn}	√	√
15	$3\frac{1}{2}$			√	√		I_d	√	√
16	5	270	270				V_n	√	√
17	5	300	300	√	√		V_n	√	√

Convergence of a.c. mismatches and d.c. residuals is to 0·001 p.u.
P_{dm1} and P_{dm2} are powers in MW
Case 16 is for Benmore generator busbars isolated from the South Island system, using simplified three-terminal model
Case 17 as for case 1 using simplified three-terminal model of d.c. link. Identical results obtained

Table 3
DIMENSIONS OF A.C. DATA FOR THE COMPLETE NEW ZEALAND NETWORK

System	Busbars	Lines	Transformers
South Island	191	113	131
North Island	341	216	273
Total	532	329	404

Table 4
SOLUTION TIMES FOR COMPLETE NEW ZEALAND NETWORK AT PEAK DAYTIME LOAD CONDITIONS

(a) Time, s	A.C. system	A.C.-d.c. system
Total solution	56	60
A.C. data input	10	10
D.C. data input	–	0·2
Triangulate B'	12	12
Triangulate B''	11	10
Iteration loop	11	16
A.C. output	11	11
D.C. output	–	0·2

(b) Typical iteration times	$P-\theta$	$Q-V$	$P-\theta$	$Q-V$
Total	0·91	0·89	1·22	1·28
Calculate a.c. mismatches	0·41	0·41	0·41	0·41
Calculate d.c. residuals and d.c. Jacobian matrix	–	–	0·06	0·06
Forward reduction of a.c. residual vector	0·14	0·13	0·15	0·15
Solution of $R = A\Delta x$ and updating of d.c. variables	–	–	0·25	0·32
Back substitution for increments in a.c. variables and updating voltages	0·36	0·35	0·35	0·34
Number of iterations	6		6	

Similar times were recorded for the full N.Z. system under light-load conditions. The number of iterations to solution was $5\frac{1}{2}$ for both a.c. and a.c.-d.c. loadflows
Burroughs B6718 digital computer used

The interface equations at Haywards remain the same as for the general model, since this end of the link has not been modified. For each of the Benmore terminals, however, only the real-power mismatch equation is available, as real power is specified. Since the generator voltages are adjusted to maintain power through the d.c. link, and since this is done by altering the reactive-power generation, the following equations and variables are used in the B'' matrix:

$$P_{dm1} - V_{dm1} I_d = 0 \quad \text{(against variable } \Delta V_{m1})$$

$$P_{dm2} - V_{dm2} I_d = 0 \quad \text{(against variable } \Delta V_{m2})$$

The resulting a.c.-d.c. Jacobian matrix equations are shown in Fig. 6, where

(i) subscript i denotes elements of the North Island a.c. system $i \neq n$

(ii) shaded areas denote zero elements.

Variables θ_{m1} and θ_{m2} are redundant in this isolated case. However, the simplified model of the d.c. link can be used equally well for the full New Zealand system, where real and reactive power generation is available on both generator busbars and the interconnecting transformer taps are fixed from South Island a.c. considerations. In this case, the transformers become part of the a.c. system, and the interface equations remain the same as for the isolated case with θ_{m1} and θ_{m2} referred to the a.c.-system slack busbar.

6 Results

Multiple cases of the New Zealand system a.c.-d.c. load flow were run on a Burroughs B6718 digital computer. Convergence of both a.c. and d.c. residuals with a tolerance of 0·001 p.u. was achieved for all feasible operating conditions tested. A summary of test cases with reduced North Island and South Island a.c. systems is given in Table 2.

Full results were also obtained for the complete N.Z. a.c. system under peak daytime load (case 1) and light night-time loading conditions (case 6). Table 3 gives the dimensions of the a.c. data and Table 4 the computing times taken for the a.c. and a.c.-d.c. load-flow solutions, respectively. For the a.c. solution, the d.c. equations were suppressed and the link represented as two load busbars, one at Benmore and the other at Haywards.

The times taken by the a.c. system solution vary little from case to case. Increases due to the d.c. link are most significant in the solution of the nonsymmetric d.c. Jacobian matrix equation.

The number of iterations required for the solution of the a.c.-d.c. load flow is the same as for the a.c. system only. Because the d.c. equations are used at every half iteration of the fast-decoupled algorithm, convergence of the d.c. residuals is rapidly achieved (two iterations in these cases).

The array-storage increases, due to the d.c. link, are also relatively small. The requirements are that there be three real vectors, one integer vector and one double-subscript array, all of dimensions N_{dc}, which is the number of d.c. equations plus the number of interface equations. For the general model described in Section 3, where $N_{dc} = 39$, the array storage is 1677 words. The combined New Zealand system of 532 busbars required 28 728 words of array storage, and the increase due to the d.c. link is only 5·8%.

7 Conclusions

Based on the N.Z. a.c.-d.c. system, a comprehensive steady-state d.c. model has been developed which includes all the convertor-related plant components found in existing d.c. links. The model in its totality represents a three-terminal series interconnection between two separate a.c. systems with nonsymmetrical pole configuration and control. With various degrees of simplification the model can also accommodate a balanced pole operation, a three-terminal d.c. configuration, and a point-to-point d.c. interconnection within a single a.c. system. Further terminals and different d.c. configurations, although not seriously considered at present, can easily be added.

The d.c. model is integrated with a fast-decoupled a.c. load flow without being reduced in convergence ability for all the practical operating conditions of the New Zealand system.

8 Acknowledgments

The authors are grateful to P.W. Blakeley, General Manager of the New Zealand Electricity Department, for his permission to publish this information, and to the Computer Centre of the University of Canterbury, New Zealand, for their help.

9 References

1 BRAUNAGEL, D.A., KRAFT, L.A., and WHYSONG, J.L.: 'Inclusion of d.c. convertor and transmission equations directly in a Newton power flow', *IEEE Trans.*, 1976, **PAS-95**, pp. 76–88
2 SATO, H., and ARRILLAGA, J.: 'Improved load-flow techniques for integrated a.c.-d.c. systems', *Proc. IEE*, 1969, **116**, (4), pp. 525–532
3 REEVE, J., FAHMY, G., and STOTT, B.: 'Versatile load-flow method for multi-terminal h.v. d.c. systems'. Presented at IEEE, PES Summer Meeting Portland, Ore., July 1976, Paper F76 354-1
4 STOTT, B.: 'Loadflows for AC and integrated AC/DC systems'. Ph.D. thesis, University of Manchester, 1971
5 ARRILLAGA, J., and BODGER, P.: 'Integration of h.v. d.c. links with fast-decoupled load-flow solutions', *Proc. IEE.*, 1977, **124**, (5), pp. 463–468
6 STOTT, B., and ALSAC, O.: 'Fast-decoupled load flow', *IEEE Trans.*, 1974, **PAS-93**, pp. 859–869

10 Appendix

Ordering of d.c. link residuals and variables

Residual		Variable
R_1	$= V_{dm1} - K_1 E_{m1} \cos \phi_{m1}$	E_{m1}
R_2	$= V_{dm2} - K_1 E_{m2} \cos (\phi_{m2} - \omega_{m2})$	E_{m2}
R_3	$= V_{dn} - K'_1 E_n \cos \phi_n$	E_n
R_4	$= K_1 I_d - a_{m1} B_m (a_{m1} E_{m1} \sin \phi_{m1} - V_{m1} \sin \psi_{m1})$	ϕ_{m1}
R_5	$= K_1 I_d \cos \omega_{m2} - a_{m2} B_m (a_{m2} E_{m2} \sin \phi_{m2} - V_{m2} \sin \psi_{m2})$	ϕ_{m2}
R_6	$= K'_1 I_d + B_{sn} (E_n \sin \phi_n - V_{in} \sin \psi_{in})$	ϕ_n
R_7	$= V_{dm1} - K_1 E_{m1} \cos \alpha_{m1} + K_2 X_{m1} I_d$	V_{dm1}
R_8	$= V_{dm2} - K_1 E_{m2} \cos \alpha_{m2} + K_2 X_{m2} I_d$	V_{dm2}
R_9	$= V_{dn} - K'_1 E_n \cos \alpha_n + K'_2 X_n I_d$	V_{dn}
R_{10}	$= \Delta P_{in}/V_{in}$	ψ_{in}
R_{11}	$= \Delta Q_{in}/V_{in}$	V_{in}
R_{12}	$= \Delta P_{tn}/V_{tn}$	ψ_{tn}
R_{13}	$= \Delta P_{im1}/V_{im1}$	ψ_{im1}
R_{14}	$= \Delta Q_{im1}/V_{im1}$	V_{im1}
R_{15}	$= \Delta P_{im2}/V_{im2}$	ψ_{im2}
R_{16}	$= \Delta Q_{im2}/V_{im2}$	V_{im2}
R_{17}	$= \Delta P_{tm1}/V_{tm1}$	ψ_{tm1}
R_{18}	$= \Delta P_{tm2}/V_{tm2}$	ψ_{tm2}
R_{19}	$= \Delta P_{m1}/V_{m1}$	ψ_{m1}
R_{20}	$= \Delta P_{m2}/V_{m2}$	ψ_{m2}
R_{21}	$= a_{m1} V_{dm1} - K_1 V_{m1} \cos \psi_{m1}$	ψ_m
R_{22}	$= K_1 I_d \sin \omega_{m2} + a_{m2} B_m (a_{m2} E_{m2} \cos \phi_{m2} - V_{m2} \cos \psi_{m2})$	ω_{m2}
R_{23}	$= V_{dn} - K'_1 V_{in} \cos \psi_{in}$	ψ_n
R_{24}	$= V_{dm1} + V_{dm2} - V_{dn} - R_{dc} I_d$	I_d
R_{25}	$= \cos \alpha^{sp}_{m1} - \cos \alpha_{m1}$	$\cos \alpha_{m1}$
R_{26}	$= \cos \alpha^{sp}_{m2} - \cos \alpha_{m2}$	$\cos \alpha_{m2}$
R_{27}	$= \cos \alpha^{sp}_{n} - \cos \alpha_{n}$	$\cos \alpha_n$
R_{28}	$= a^{sp}_{m1} - a_{m1}$	a_{m1}
R_{29}	$= a^{sp}_{m2} - a_{m2}$	a_{m2}
R_{30}	$= a^{sp}_{n} - a_{n}$	a_n
R_{31}	$= t^{sp}_{m1} - t_{m1}$	t_{m1}
R_{32}	$= t^{sp}_{m2} - t_{m2}$	t_{m2}
R_{33}	$= P_{dm1} - V_{dm1} I_d$	V_{m1}
R_{34}	$= P_{dm2} - V_{dm2} I_d$	V_{m2}
R_{35}	$= \Delta Q_{tm1}/V_{tm1}$	V_{tm1}
R_{36}	$= \Delta Q_{tm2}/V_{tm2}$	V_{tm2}
R_{37}	$= V^{sp}_{n} - V_n$	V_{tn}

control equations are for case 1 of results.